Research Article | Vol. 25, No. 11 | 29 May 2017 | OPTICS EXPRESS 12675
Optics EXPRESS

Experimental and numerical study of the nonlinear response of optical multilayers

TATIANA AMOTCHKINA,[1] MICHAEL TRUBETSKOV,[1] AND VLADIMIR PERVAK[2,*]

[1]*Max-Planck-Institut für Quantenoptik, Hans-Kopfermann str. 1, 85748 Garching, Germany*
[2]*Ludwig-Maximilians-Universität München, Am Coulombwall 1, 85748 Garching, Germany*
[*]*Vladimir.Pervak@lmu.de*

Abstract: Dielectric multilayer coatings exhibiting steep reflectance in an extremely narrow transition zone, highly sensitive to any variations of layer refractive indices and therefore suitable for studying the nonlinear properties are produced and characterized. Increase of reflectance at growing intensity reveals the presence of the optical Kerr effect. A new method calculating intensity dependent spectral characteristics of multilayer optical coatings in the case of nonlinear interaction with high intensity laser pulses is developed. The method is based on the numerical solution of a boundary-value problem derived from the system of Maxwell equations describing the propagation of light through a multilayer system. The method opens a way to synthesis of optical coatings with predictable nonlinear properties. Comparison of our numerical modelling with experimental data enabled us to accurately determine the Kerr coefficients n_2 of the widely-used thin-film materials Ta_2O_5 and Nb_2O_5.

OCIS codes: (310.4165) Multilayer design; (310.1620) Interference coatings; (310.6860) Thin films, optical properties; (320.7110) Ultrafast nonlinear optics.

References and links

1. V. Pervak, O. Razskazovskaya, I. B. Angelov, K. L. Vodopyanov, and M. Trubetskov, "Dispersive mirror technology for ultrafast lasers in the range 220–4500 nm," Adv. Opt. Technol. **3**, 55–63 (2014).
2. O. Razskazovskaya, F. Krausz, and V. Pervak, "Multilayer coatings for femto- and attosecond technology," Optica **4**(1), 129 (2017).
3. H. A. Macleod, *Thin-Film Optical Filters*, 4th ed. (Taylor and Francis, 2010).
4. I. B. Angelov, M. von Pechmann, M. K. Trubetskov, F. Krausz, and V. Pervak, "Optical breakdown of multilayer thin-films induced by ultrashort pulses at MHz repetition rates," Opt. Express **21**(25), 31453–31461 (2013).
5. K. Starke, D. Ristau, H. Welling, T. V. Amotchkina, M. Trubetskov, A. A. Tikhonravov, and A. S. Chirkin, "Investigations in the nonlinear behavior of dielectrics by using ultrashort pulses (Best Oral Presentation)," Proc. SPIE **5273**, 501 (2004).
6. M. Mero, J. Liu, W. Rudolph, D. Ristau, and K. Starke, "Scaling laws of femtosecond laser pulse induced breakdown in oxide films," Phys. Rev. B **71**(11), 115109 (2005).
7. M. Mero, J. Liu, A. Sabbah, J. C. Jasapara, K. Starke, D. Ristau, J. K. McIver, and W. G. Rudolph, "Femtosecond pulse damage and predamage behavior of dielectric thin films," Proc. SPIE **4932**, 202 (2003).
8. L. A. Emmert, C. Rodriguez, Z. Sun, F. Beygi Azar Aghbolagh, S. Günster, D. Ristau, D. Patel, C. S. Menoni, and W. Rudolph, "Optical coatings excited by femtosecond lasers near the damage threshold: challenges and opportunities," Proc. SPIE **9632**, 96320K (2015).
9. C. Rodríguez, S. Günster, D. Ristau, and W. Rudolph, "Frequency tripling mirror," Opt. Express **23**(24), 31594–31601 (2015).
10. O. Razskazovskaya, T. T. Luu, M. Trubetskov, E. Goulielmakis, and V. Pervak, "Nonlinear absorbance in dielectric multilayers," Optica **2**(9), 803 (2015).
11. E. Fedulova, M. Trubetskov, T. Amotchkina, K. Fritsch, P. Baum, O. Pronin, and V. Pervak, "Kerr effect in multilayer dielectric coatings," Opt. Express **24**(19), 21802–21817 (2016).
12. T. Amotchkina, M. K. Trubetskov, E. Fedulova, K. Fritsch, O. Pronin, F. Krausz, and V. Pervak, "Characterization of nonlinear effects in edge filters," in *Optical Interference Coatings 2016*, OSA Technical Digest (online) (Optical Society of America, 2016), paper ThD.3.
13. B. G. Bovard and H. A. Macleod, "Nonlinear behaviour of optical coatings subjected to intense laser irradiation," J. Mod. Opt. **35**(7), 1151–1168 (1988).
14. T. A. Laine and A. T. Friberg, "Nonlinear thin-layer theory for stratified Kerr medium," Appl. Phys. Lett. **74**(22), 3248–3250 (1999).
15. J. Hsu, C. Fuentes-Hernandez, A. R. Ernst, and B. Kippelen, "Ultrafast nonlinear mirrors with broad spectral and angular bandwidths in the visible spectral range," Opt. Express **21**(3), 3573–3581 (2013).
16. N. Katte, J. W. Haus, P. Powers, A. Sarangan, J. Gao, and M. Scalora, "Third-order nonlinear optical properties of metallodielectric stacks," J. Opt. Soc. Am. B **28**(9), 2277 (2011).

#291663 https://doi.org/10.1364/OE.25.012675
Journal © 2017 Received 28 Mar 2017; revised 12 May 2017; accepted 14 May 2017; published 22 May 2017

Optics EXPRESS

17. D. T. Owens, C. Fuentes-Hernandez, J. M. Hales, J. W. Perry, and B. Kippelen, "Nonlinear optical properties of induced transmission filters," Opt. Express **18**(18), 19101–19113 (2010).
18. M. Sheik-Bahae and P. Michael, Hasselbeck, "Third-order optical nonlinearities" in *Handbook of Optics* Vol. IV, M. Bass, ed. (McGraw-Hill, 2010).
19. S. A. Furman and A. V. Tikhonravov, *Basics of Optics of Multilayer Systems* (Editions Frontières, 1992).
20. R. Adair, L. L. Chase, and S. A. Payne, "Nonlinear refractive index of optical crystals," Phys. Rev. B Condens. Matter **39**(5), 3337–3350 (1989).
21. V. Dimitrov and S. Sakka, "Linear and nonlinear optical properties of simple oxides. II," J. Appl. Phys. **79**(3), 1741–1745 (1996).
22. M. L. Gorodetsky, "Thermal noises and noise compensation in high-reflection multilayer coating," Phys. Lett. A **372**(46), 6813–6822 (2008).
23. M. Evans, S. Ballmer, M. Fejer, P. Fritschel, G. Harry, and G. Ogin, "Thermo-optic noise in coated mirrors for high-precision optical measurements," Phys. Rev. D Part. Fields Gravit. Cosmol. **78**(10), 102003 (2008).
24. T.-C. Chen, C.-J. Chu, C.-H. Ho, C.-C. Wu, and C.-C. Lee, "Determination of stress-optical and thermal-optical coefficients of Nb2O5 thin film material," J. Appl. Phys. **101**(4), 043513 (2007).
25. A. V. Tikhonravov and M. K. Trubetskov, "OptiLayer software," http://www.optilayer.com.
26. A. V. Tikhonravov, M. K. Trubetskov, and G. W. DeBell, "Optical coating design approaches based on the needle optimization technique," Appl. Opt. **46**(5), 704–710 (2007).
27. V. Pervak, A. V. Tikhonravov, M. K. Trubetskov, S. Naumov, F. Krausz, and A. Apolonski, "1.5-octave chirped mirror for pulse compression down to sub-3 fs," Appl. Phys. B **87**(1), 5–12 (2007).
28. T. V. Amotchkina, A. V. Tikhonravov, M. K. Trubetskov, D. Grupe, A. Apolonski, and V. Pervak, "Measurement of group delay of dispersive mirrors with white-light interferometer," Appl. Opt. **48**(5), 949–956 (2009).
29. I. Balasa, L. O. Jensen, and D. Ristau, "Laser calorimetric absorptance testing of samples with varying geometry," Opt. Eng. **53**(12), 122503 (2014).
30. W. Schneider, A. Ryabov, C. Lombosi, T. Metzger, Z. Major, J. A. Fülöp, and P. Baum, "800-fs, 330-µJ pulses from a 100-W regenerative Yb:YAG thin-disk amplifier at 300 kHz and THz generation in $LiNbO_3$," Opt. Lett. **39**(23), 6604–6607 (2014).
31. J. Bonse, S. Baudach, J. Krueger, W. Kautek, K. Starke, T. Gross, D. Ristau, W. G. Rudolph, J. C. Jasapara, and E. Welsch, "Femtosecond laser damage in dielectric coatings," Proc. SPIE **4347**, 24 (2001).
32. C.-Y. Tai, J. Wilkinson, N. Perney, M. Netti, F. Cattaneo, C. Finlayson, and J. Baumberg, "Determination of nonlinear refractive index in a Ta2O5 rib waveguide using self-phase modulation," Opt. Express **12**(21), 5110–5116 (2004).

1. Introduction

Dielectric optical coatings play an extremely important role in pushing frontiers of femtosecond and attosecond laser technology. Currently, the majority of ultrafast lasers include multilayer optical elements providing accurate group delay/group delay dispersion control as well as desired spectral characteristics [1,2]. Consideration of these multilayers is performed in the frame of a linear theory of optical coatings that is well-known and widely used [3]. Nonlinear interactions of ultrashort pulses with dielectric optical coatings have been studied in the context of laser-induced damage, as an effect that should be minimized [4–7]. In [8] the qualitative behavior of optical multilayers has been categorized in four fluence ranges. At low intensities (i), the interaction of a laser pulse with a coating can be described in the frame of the linear model. With growing pulse intensity (ii), nonlinear effects such as the optical Kerr effect come into play due to anharmonicity of the materials' polarization response. Approaching the optical breakdown threshold (iii), higher-order nonlinear effects such as multi-photon and tunnel ionization, resultant hot electron (plasma) formation in the conduction band possibly accompanied by impact ionization tend to set in. Beyond the breakdown threshold (iv), irreversible modifications occur.

In the intensity ranges (ii) and (iii), exploitation or suppression of the emerging nonlinear effects may be desirable. For instance, in [9] a frequency tripling mirror producing third harmonic in reflection was designed and fabricated. In [10] the performance of dispersive mirrors was improved due to analyzing and minimizing two-photon absorption. In [11,12] it was reported on specially-designed edge filters exhibiting a pronounced sensitivity to the nonlinear Kerr effect, which may potentially be exploited for laser mode locking.

So far, only few models describing propagation of high intensity electromagnetic fields through dielectric multilayers were considered. In [13] a thermo-optic model and its modification admitting nonlinear refractive indices was developed. Simulations of thermo-optic effects as well as nonlinear effects of a quarter wave stack containing 401

Optics EXPRESS

thin layers were provided. In [14] a model valid for a specific case only was developed, namely, nonlinearities in layers with thicknesses which are small as compared to the wavelength were assumed. In [15–17] heterogeneous structures containing metal films were considered. In particular, nonlinear optical properties of a mirror comprising of a 100 nm Ag reflector with a 23 nm Au layer sandwiched between two SiO_2 layers was studied [15]. Third-order nonlinear properties of Ag-TiO_2 metal-dielectric stacks were investigated [16]. In [17] the nonlinear optical properties of Ag/Ta_2O_5/SiO_2 filters were experimentally studied and simulation of their properties was provided. It was assumed that the energy was absorbed by the multilayer and converted directly to the heat in the metal layer. The layer parameters were then recalculated with the help of temperature-dependent Drude parameters and changes of the coating's spectral characteristics were extracted. In [10] a theoretical model allowing estimation of the two-photon absorption coefficient and predicting intensity dependent behavior of multilayer coatings was proposed. In this model, the incident radiation is supposed to be s-polarized that simplifies significantly solving a system of differential equations describing the propagation of light through a multilayer coating.

In [12] a nonlinear increase of the reflectance was considered in the frame of a simplified model assuming that the nominal refractive index of high index layers equals to n_H at low intensities and to the intensity dependent effective refractive index $\tilde{n}_H$

$$\tilde{n}_H = n_H + n_2 I \tag{1}$$

at high intensities [18]. In Eq. (1), n_2 is a Kerr coefficient, I is the light intensity. The intensity dependent spectral characteristics $R(I), T(I)$ were calculated with the help of the well-known linear theory (see, for example [3,19],). This simplified model does not take the dependence of the nonlinear refractive index on layer coordinate into account.

Up to now, a universal method of evaluation of intensity dependent reflectance and transmittance of dielectric multilayer coatings is not available. Hence, it was not possible to incorporate the nonlinear Kerr effect into multilayer design and analysis. In addition, Kerr coefficients of thin dielectric layers have not been reliably determined. These coefficients may differ significantly from the Kerr coefficients of the same materials in the bulk form. The latter coefficients can be found in the literature [20,21].

The primary goal of this work is to propose a mathematical model of nonlinear optical multilayers and establish a numerical method for the accurate description of the nonlinear response of multilayer coatings to strong laser fields. The calculation of intensity-dependent reflectance and transmittance $R(I)$ and $T(I)$ had to be validated by the experimental data. The secondary goal was to determine the Kerr coefficients of two thin film dielectric materials, Ta_2O_5 and Nb_2O_5 with the help of the new method. The experimental data used for the validation of the model calculations as well as for the determination of n_2 values of thin film materials was obtained with the help of carefully developed measurement process. This data includes reflectance and transmittance values measured at the increasing intensities as well as at different incidence angles. The measurements were built with a specially built laser setup based on an Yb:YAG thin disk amplifier.

In Section 2, the design, production and optical characterization of nonlinear multilayers (NMC) is presented. In addition to the results presented in [11], careful optical characterization of the manufactured coatings was performed in this work to be able to put our model calculations to the test as precisely as possible. In Section 3, the results of nonlinear characterization of the produced NMCs with the help of ultrashort laser pulses are described. The measurement process was modified as compared to [11] in a non-destructive way that allowed detecting pre-damage behavior of investigated samples. In Section 4, a new numerical method of calculation of intensity-dependent spectral characteristics is provided. In Section 5, results of model calculations are compared with experimental data and Kerr coefficients of two thin film materials are estimated. Conclusions are presented in Section 6.

Optics EXPRESS

2. Design, production and optical characterization of nonlinear coatings

Since the Kerr coefficients of dielectric materials are small enough, the spectral characteristics of the NMC designs need to be very sensitive to even small refractive index variations. For this purpose edge filters with extremely narrow transition zone between high and low reflectance ranges around the laser central wavelength of 1030 nm were proposed. The idea of the nonlinear multilayer design is illustrated in Fig. 1(a). It is expected that with the increasing intensity refractive indices of layers grow (Eq. (1)), the nominal reflectance curve $R_0(\lambda)$ is shifted to the longer wavelengths ($R_{nl}(\lambda)$ in Fig. 1(a)) and reflectance value at the central wavelength increases by the *modulation depth* ΔR. In Fig. 1(a) $R_{nl}(\lambda)$ illustrates shifted reflectance of the filter at high intensity values.

Two pairs of thin film materials were used in the design process, namely Nb_2O_5/SiO_2 and Ta_2O_5/SiO_2; the substrate was made of fused silica. Nominal refractive indices of the thin film materials and the substrate were specified by the Cauchy formula:

$$n(\lambda) = A_0 + A_1\left(\frac{\lambda_0}{\lambda}\right)^2 + A_2\left(\frac{\lambda_0}{\lambda}\right)^4, \tag{2}$$

where A_0, A_1, A_2 are dimensionless parameters, $\lambda_0 = 1000\text{nm}$ and λ is specified in nanometers.

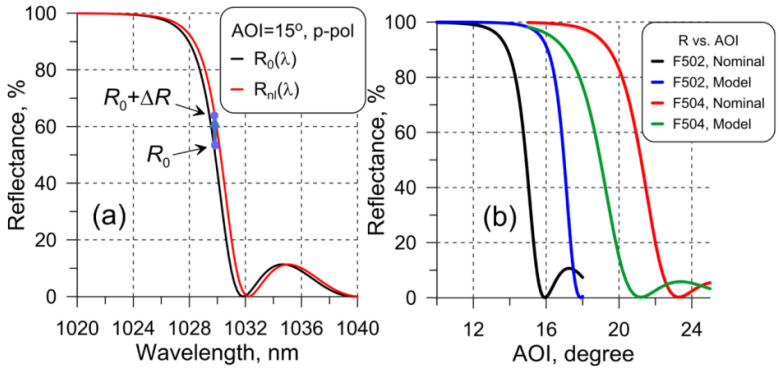

Fig. 1. (a) Sensitivity of the NMC reflection to a small increase of refractive index (see the text for details); (b) Angular reflectance sensitivity of the designed and produced NMCs.

Cauchy parameters describing dispersion behavior of refractive indices of thin film materials and substrates used in the designs are presented in Table 1. Designing of NMCs was performed with the help of the needle optimization technique and gradual evolution algorithm incorporated into OptiLayer Thin Film Software [25,26]. Target reflectance was 100% in the spectral range from 900 nm to 1029 nm and 0% in the range from 1031 nm to 1100 nm. In the case of Ta_2O_5/SiO_2 thin film materials, an additional requirement was introduced: the desired group delay dispersion (GDD) for the p-polarized light was -5000 fs^2 in the range from 1024 nm to 1033 nm. A merit function estimating the closeness of the designed spectral reflectance in the p-polarized case $R^{(p)}$ to the target one was defined as:

$$MF^2 = \sum_{j=1}^{134}\left(R^{(p)}(\mathbf{X};\lambda_j) - 100\%\right)^2 + \sum_{i=1}^{66}\left(R^{(p)}(\mathbf{X};\lambda_i)\right)^2, \tag{3}$$

where $\{\lambda_j\}$ and $\{\lambda_i\}$ are wavelength points in the ranges from 900 nm to 1029 nm and from 1031 nm to 1100 nm, respectively. It is seen that the width of the target transition

Optics EXPRESS

zone is only about 2 nm. In Eq. (3), $\mathbf{X}=\{d_1,...,d_m\}$ is the vector of layer thicknesses, m is the number of layers, the angle of incidence (AOI) is 15°.

In the case of Ta_2O_5/SiO_2 materials pair, a term estimating the GDD performance was added to the merit function:

$$MF^2=\sum_{j=1}^{134}\left(R^{(p)}\left(\mathbf{X};\lambda_j\right)-100\right)^2+\sum_{i=1}^{66}\left(R^{(p)}\left(\mathbf{X};\lambda_i\right)\right)^2+\sum_{k=1}^{200}\left[\frac{GDD^{(p)}\left(\mathbf{X};\lambda_k\right)+5000}{5000}\right]^2, \quad (4)$$

where $\{\lambda_k\}$ is the wavelength grid in the range from 1024 nm to 1033 nm, Δ_k are tolerances introduced to balance the reflectance and GDD target requirements. During the design process $\Delta_k=5000\ \mathrm{fs}^2$ was used.

As the result, two filter designs named F502 (materials Nb_2O_5/SiO_2) and F504 (materials Ta_2O_5/SiO_2) were obtained. The NMCs consist of 69 layers and have total physical thicknesses of 8.7 μm and 9.2 μm, respectively. The structures of the obtained designs are shown in Fig. 2. Spectral performance of F502 filter in the vicinity of the central wavelength of 1030 nm is shown in Fig. 1(a) by a black curve. The red curve in Fig. 1(a) represents reflectance of F502 filter calculated under the assumption that the refractive indices of all high index layers were increased by 0.001, i.e., for Nb_2O_5 layers $A_0=2.219485$ was taken for calculations. It is seen that even with such a small variation of the refractive index, the reflectance curve is shifted to the longer wavelengths and the modulation depth ΔR at the wavelength of 1030 nm is quite big (about 15%). It means that at high intensities, filter reflectance is expected to be increased. The actual values of the modulation depth are estimated based on the intensity measurements described in Section 3.

Table 1. Cauchy coefficients and thermo-optic parameters of layers' refractive indices and substrate.

Material	A_0	A_1	A_2	Thermal expansion coefficient, K^{-1}	Thermo-optic coefficient, K^{-1}
Ta_2O_5	2.065721	0.016830	0.001686	$3.6\cdot10^{-6}$ [22]	$6\cdot10^{-5}$ [22]
Nb_2O_5	2.218485	0.021827	0.00399968	$5.8\cdot10^{-6}$ [23]	$1.43\cdot10^{-5}$ [24]
SiO_2	1.465294	0	0.00047108	$0.51\cdot10^{-6}$ [23]	$8\cdot10^{-6}$ [23]
Fused Silica	1.443268	0.00406	$6.9481764\cdot10^{-6}$		

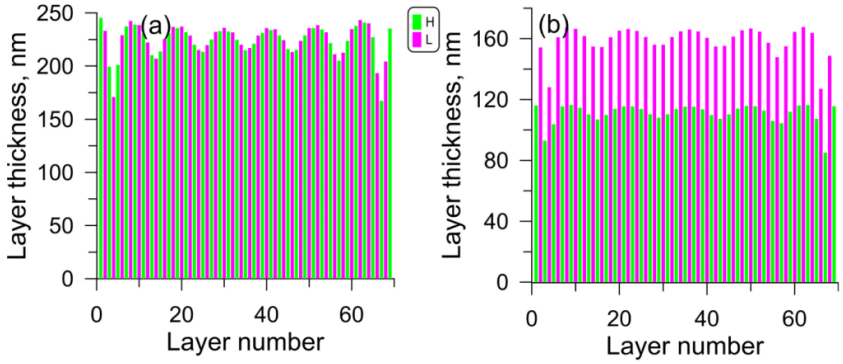

Fig. 2. Structures of the designed NMCs: F502 (a), F504 (b).

Optics EXPRESS

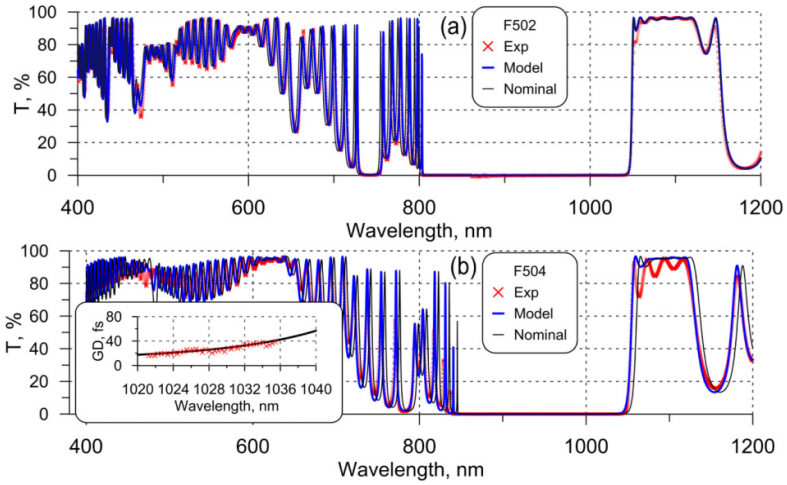

Fig. 3. Comparison of the experimental, nominal and model transmittance curves of F502 (a) and F504 (b) samples. Inset: comparison of measured and nominal group delay at AOI = 8°.

In Fig. 1(b) the nominal angular dependencies of the F502 and F504 filters are plotted. One can observe that the spectral reflectance at the wavelength of 1030 nm is extremely sensitive to the angle of incidence. For F502 filter, reflectance values R_0 vary across the range from almost 100% down to 0% when AOI varies from 12° to 16°; for F504 sample, reflectance values R_0 vary from almost 100% at AOI of 16° down to 5% at the AOI of 23°. It means that F504 filter is less sensitive to the AOI than F502 sample. This is connected with the fact that the additional requirement on GDD was specified for F504 design.

Production of the designed filters was a complicated task requiring advanced instrumental tools, high monitoring accuracy and a lot of deposition experience. The main challenge was to provide extremely steep spectral characteristics in the vicinity of the central wavelength of 1030 nm. The designed NMCs were produced using Bühler Leybold Optics magnetron sputtering Helios high vacuum coating system, the layer thicknesses were controlled with the help of well-calibrated time monitoring [27]. Substrates of different thicknesses/diameters were coated, namely 0.2 mm/10mm, 1 mm/10mm and 6.35 mm/25.4 mm.

Transmittance data of the produced samples was measured by Perkin Elmer 950 spectrophotometer in the range from 400 nm to 1200 nm. To reveal all informative features in the transmittance spectrum as well as to describe accurately the steep variations of the transmittance curve, the measurements were performed at 0.2 nm wavelength step and at the spectral resolution of 0.5 nm (Fig. 3). The slit size of 0.5 nm corresponds to the line width (optical resolution) of 0.5 nm. It means that all spectral features reveling themselves in the narrow spectral ranges of 0.5 nm width will not be clearly described. The transmittance curves of the designs considered in the present work do not contain such features. It is seen from Fig. 3 that the spectral characteristics of NMCs exhibit expected steep variations as well as all spectral features. At the same time, the measurement curves are shifted towards to the longer (F502) or shorter (F504) wavelengths with respect to the nominal ones (black curves in Fig. 3). These shifts can be addressed to presence of small systematic errors inevitable during the high vacuum coating process. For further modeling of the nonlinear effects (Section 4), it was important to know the actual design thicknesses. To estimate these thicknesses, the experimental transmittance data was to be fitted by model transmittance. For this purpose, the discrepancy function DF estimating the closeness between experimental and model spectral characteristics was to be optimized with respect to the relative systematic shifts Δ_H, Δ_L in layer thicknesses:

Optics EXPRESS

$$DF\left(\Delta_H,\Delta_L\right)=\sum_{j=1}^{L}\left[T\left(d_1\left(1+\Delta_H\right),d_2\left(1+\Delta_L\right),...;\lambda_j\right)-\hat{T}\left(\lambda_j\right)\right]^2\rightarrow\min, \qquad (5)$$

where $\hat{T}\left(\lambda_j\right)$ are measured transmittance values at the wavelength grid $\left\{\lambda_j\right\}, j=1,...,L$, T is the model transmittance. As a result, relative systematic thickness shifts in layer thicknesses were estimated equal to $n_H=0.7\%$, $n_L=0.3\%$ and $n_H=-1.4\%$, $n_L=0.3\%$ for F502 and F504 samples, respectively. Corresponding model transmittance data is shown in Fig. 3 by blue curves. It is seen that the deviations of the model transmittance curves from the experimental ones still exist in the range from 1050 nm to 1100 nm. Investigation of possible reasons of such deviations are out of scope of this paper. For model calculations provided in Section 5, F502 and F504 designs with shifted layer thicknesses $d_1\left(1+\Delta_H\right),d_2\left(1+\Delta_L\right)...,d_{69}\left(1+\Delta_H\right)$ were used.

Due to the special structure of the NMC designs, the systematic shifts Δ_H, Δ_L of layer thicknesses do not affect high sensitivity of the produced filters to the refractive index variations and the AOI. It is demonstrated in Fig. 1(b) where angular dependencies of the model and nominal reflectance are plotted. In order to achieve the steep transition zone in the experiment, the AOI should be adjusted accordingly.

The group delay of the F504 sample was measured with the help of a home-made white light interferometer [28]. Measured and nominal group delay values are in a good agreement (see the inset of Fig. 3(b)).

Absorption of the F502 sample on 6.35 mm substrate and F504 sample on a 1 mm substrate was measured using laser calorimetry [29]. The absorption values were found equal to 66 ppm (F502 sample) and 76 ppm (F504 sample). Therefore, the samples possessed a small linear absorptance and thermal effects had to be taken into account.

3. Intensity dependent measurements

The nonlinear behavior of the produced NMCs were studied with the setup shown in Fig. 4. The laser was an Yb:YAG thin-disk regenerative amplifier with a repetition rate $f_{rep}=50$ kHz emitting 1 ps pulses ($\tau_p=1$ ps) [30]. The pulse intensity was varied with a $\lambda/2$ plate followed by a polarization cube. The beam diameter (the distance from the beam axis where the intensity drops to $1/e^2$ of the maximum value) was measured in the beam focus with the help of a CCD camera. The beam size on the sample was estimated equal to 375 μm x 396 μm with the accuracy of 5%. Incident P_{inc}, reflected P_{ref} and transmitted P_{tr} power was measured with a powermeter (PM-10, COHERENT). The relative level of fluctuations shown by powermeter was estimated as 0.5%. The temperature change Δt of the spot where the laser hits the NMC sample was monitored with the help of the infrared camera (FLIR SC 300 Series Camera A325) with the accuracy of $\pm 2^0$C.

In the course of the measurement process, the incident power was increased gradually until the damage or irreversible materials' modifications occur. The damage was indicated by a rapid increase of the surface temperature and a decrease of the transmitted/reflected power. Irreversible sample modifications revealed themselves in strong fluctuations of the transmitted/reflected power simultaneously with decreasing this power. A charge-coupled device camera monitored the sample surface. The camera was used for additional control of a strong escalation of the scattered light indicating damage occurrence [31].

The NMC samples were placed in the beam focus on a rotational stage in order to adjust the AOI and achieve different initial reflectance $\left(R_0\right)$ and transmittance $\left(T_0\right)$ levels (see Fig. 1(b)). Reflectance and transmittance coefficients of the NMC were estimated as follows:

Optics EXPRESS

$$R = \frac{P_{ref}}{P_{inc}}, \quad T = \frac{P_{tr}}{P_{inc}}. \tag{6}$$

The peak intensity I of the Gaussian pulse was calculated as:

$$I = \frac{2P_{inc}}{f_{rep}\tau_p \pi ab}, \tag{7}$$

where a, b are radii of the Gaussian beam. In the experiment $a \approx 187.5\,\mu m$, $b \approx 198\,\mu m$.

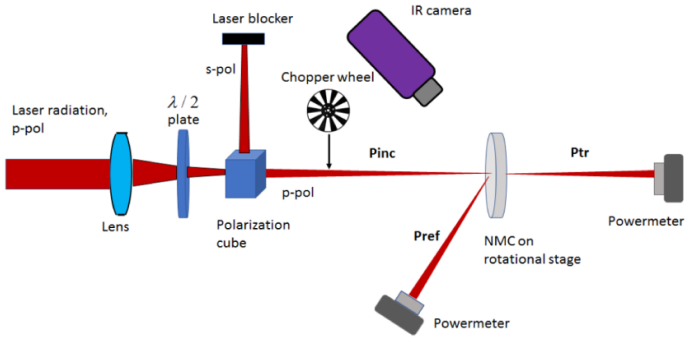

Fig. 4. Schematic of the setup for studying the nonlinear effects of the NMC samples. Yb:YAG thin-disk regenerative amplifier: 1030 nm central wavelength, 50 kHz repetition rate, 1 ps pulse duration [30].

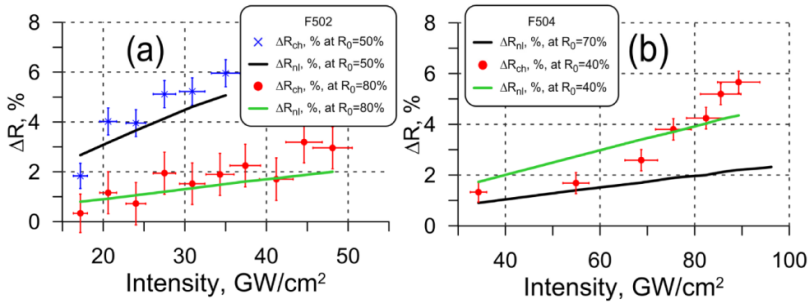

Fig. 5. Comparison of experimental modulation depths values measured with optical chopper at increasing intensities and model values calculated with the help of the developed method (see the details in Section 4): F502 (a), F504 (b).

The initial R_0, T_0 values were adjusted at a small incident power value $P_{inc} = 200\,mW$ corresponding the intensity of 6.7 GW/cm^2. It was assumed that at this intensity level nonlinear effects in dielectric layers are negligible. For each R_0, a series of $R(I)$ values was measured. After each I increase, the incident power of 200 mW was set up again and it was checked that the values R_0, T_0 were not changed. This can serve as a verification that no long-live or irreversible modifications of the layer materials occurred.

It was noticed in the course of these and previous similar intensity measurements [11] that the surface temperature grows with the increasing intensity. The temperature growth can be explained by the presence of absorption in produced coatings. Due to the temperature increase coatings' layers become thicker because of the thermal expansion and the refractive indices grow because of the thermo-optic effect. Thus, optical thicknesses of the layers increase and the spectral characteristics shift to the longer wavelengths that leads in its turn to the increase of reflectance at the wavelength of 1030 nm. In order to decouple the thermal and nonlinear effects experimentally, a chopper wheel (10% duty cycle) was inserted into the measurement setup (Fig. 4). When the laser

Optics EXPRESS

beam is modulated by the chopper wheel, the incident average power decreases approximately by 10 times without attenuating the peak intensity which drives the nonlinear process (Eq. (7)). It was noticed that when the chopper wheel was switched on, the temperature increase was not observed at all or was only 1-2°C at high intensities close to the damage.

At each intensity value, the incident $P_{inc,ch}$, reflected $P_{ref,ch}$ and transmitted $P_{tr,ch}$ power values with switched chopper were recorded. In this case, the reflectance R_{ch} and transmittance T_{ch} of the NMC samples were estimated as:

$$R_{ch} = \frac{P_{ref,ch}}{P_{inc,ch}}, \quad T_{ch} = \frac{P_{tr,ch}}{P_{inc,ch}}. \tag{8}$$

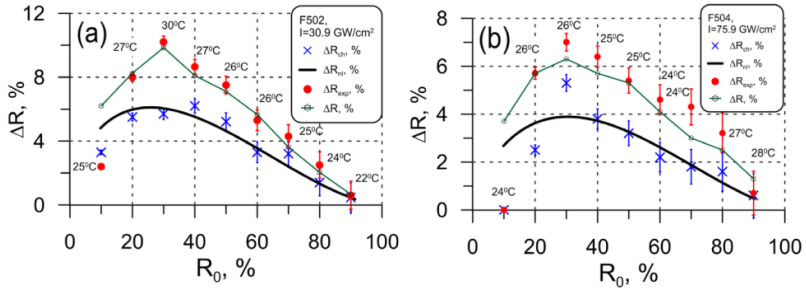

Fig. 6. Comparison of the experimental modulation depth values measured at different R_0 levels and modulation depths calculated based on the developed model (see Sections 4 and 5 for details).

In Fig. 5 modulation depth values $\Delta R_{ch}(I) = R_{ch}(I) - R_0$ measured at different intensities are presented. In Fig. 5(a) the experimental values corresponding F502 sample and the reflectance levels of 50% and 80% are shown. Figure 5(b) represents ΔR_{ch} values of F504 sample measured at the reflectance levels $R_0 = 40\%, R_0 = 70\%$. The increase of the modulation depth with growing intensity is clearly observed.

In Fig. 6 the modulation depth values at different R_0 levels (different AOI) measured when the optical chopper was switched on (ΔR_{ch}, blue crosses) and when the optical chopper was switched off ($\Delta R_{\exp}$, red spots) are presented. In the case of F502 sample, the values measured at the intensity level of 30.9 GW/cm^2 are collected and in the case of F504 sample, the experimental values corresponding to the intensity of 75.9 GW/cm^2 are shown. The temperature values recorded in the course of the measurements without optical chopper are indicated. In Section 5, the experimental values are fitted by the model dependencies $\Delta R_{nl}(I)$, $\Delta R(R_0)$, and $\Delta R_{nl}(R_0)$ (solid curves in Figs. 5 and 6).

4. Method for the evaluation of design spectral characteristics in the nonlinear case

The optical Kerr-effect in NMCs can be described as an induced addition to the refractive index proportional to the squared modulus of the electric field amplitude:

$$\Delta n(z) = n_2 I(z), \quad I = \frac{|\mathbf{E}(z)|^2}{2\eta_0}, \tag{9}$$

where z is the coordinate along the coating's cross section, $\eta_0 = 376.7\Omega$ is the impedance of vacuum, the electric field is measured in V/cm and the pulse intensity is measured in W/cm^2, n_2 is measured in cm^2/W. Three assumptions were done for the present model calculations:

Optics EXPRESS

- The calculations were carried out in the approximation of plane quasi-monochromatic waves assuming that the pulse bandwidth $\Delta\omega$ is much less than the carrier frequency ω_0, or, in terms of a time scale, that the pulse duration τ_p is much longer than the optical period $2\pi/\omega_0$. Actually, the bandwidth of the pulses used in the experiment is about 3.4 nm, $\Delta\omega = 3.55$ THz $\omega_0 = 1830$ THz; the optical period of 1.3 fs is much shorter than the pulse duration $\tau_p = 1$ ps.

- Since Kerr coefficient of SiO_2 is significantly less than n_2 of Ta_2O_5 and Nb_2O_5 [20], then the induced addition Δn in SiO_2 layers was neglected.

- Absorption was neglected in the course of the model calculations. This assumption does not limit the applicability of the model.

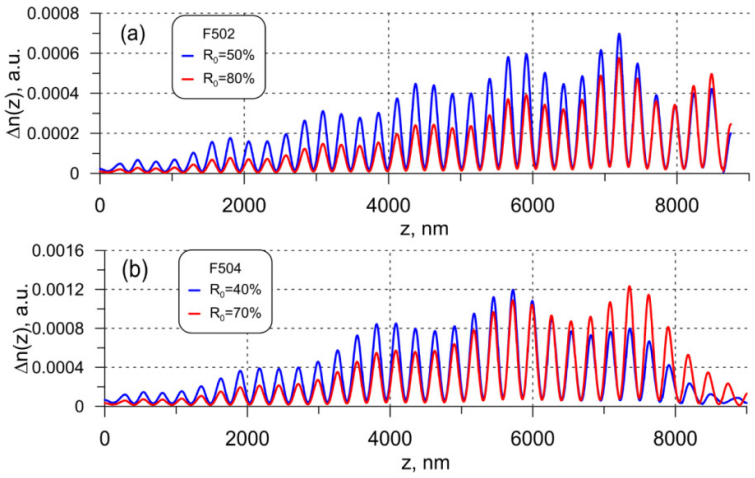

Fig. 7. Nonlinear addition to the refractive index $\Delta n(z)$ (Eq. (9)) calculated for F502 design at the intensity of 30.9 GW/cm^2, reflectance levels R_0 of 50% and 80% (a) and for F504 design at the intensity of 75.9 GW/cm^2, reflectance levels R_0 of 40% and 70% (b).

The initial system of Maxwell equations describing the interaction of *p*-polarized light with a multilayer coating can be reduced to a Cauchy problem for a system of two nonlinear ordinary differential equations by the analogy with [19]:

$$\frac{du}{dz} = ik\left[1 - \frac{\alpha^2}{\tilde{n}^2\left(z, |\mathbf{E}(z)|\right)}\right]v, \quad \frac{dv}{dz} = ik\tilde{n}^2\left(z, |\mathbf{E}(z)|\right)u, \quad 0 < z < z_a,$$

$$\tilde{n}\left(z, |\mathbf{E}(z)|\right) = n(z) + n_2|\mathbf{E}(z)|^2, \quad \mathbf{E}(z) = \left\{u(z); -\frac{\alpha\, v(z)}{\tilde{n}^2\left(z, |\mathbf{E}(z)|\right)}\right\}, \qquad (10)$$

$$u(0) = E_T, \quad v(0) = q_s E_T,$$

where E_T is the amplitude of the tangential component of the electric vector of the transmitted wave at the boundary with the substrate, $q_s = n_s^2/\sqrt{n_s^2 - \alpha^2}$, $\alpha = n_a \sin\theta$, n_s is the refractive index of the substrate, n_a is the refractive index of the incident medium, θ is AOI. In Eq. (10), $k = 2\pi/\lambda$ is the wavenumber, $u(z)$ and $v(z)$ are tangential

Optics EXPRESS

amplitudes of the electric and magnetic fields, respectively, and $\tilde{n}(z)$ is the nonlinear refractive index profile of the multilayer design and $E(z)$ is the full electric field. The coordinate $z=0$ corresponds to the boundary between the coating and the substrate, and the coordinate z_a corresponds to the boundary between the coating and the ambient medium.

In the linear case, the scaling of the equations is done with respect to $E_T=1$ [19]. This allows one to express amplitudes of the incident (E_A) and reflected (E_R) fields through the solutions of Eq. (10) with initial conditions related to $E_T=1$:

$$E_R=\frac{q_a u(z_a,k)-v(z_a,k)}{2q_a},\ E_A=\frac{q_a u(z_a,k)+v(z_a,k)}{2q_a}. \tag{11}$$

Then reflectance of the multilayer coating can be expressed as:

$$R(E_A,k)=\left|\frac{q_a u(z_a,k)-v(z_a,k)}{q_a u(z_a,k)+v(z_a,k)}\right|^2. \tag{12}$$

In Eqs. (11) and (12) $q_a=1/\cos\theta$. Note that the model Eq. (10) differs from the one in [10] by considering *p*-polarization case, when electric field vector has two non-zero components. It makes the introduction of nonlinear refractive index modulation more complicated.

The scaling with respect to E_T cannot be done in the nonlinear case (*p*-polarization) because the full electric field $E(z)$ is included in Eq. (10). The amplitude of the incident electric field E_A depends on the amplitude of the transmitted field in a nonlinear way:

$$E_A=f(E_T), \tag{13}$$

where f represents the solution of Eqs. (10) and (11). This solution can be found by considering various E_T values, calculating corresponding $u(z),v(z),E(z),\tilde{n}(z),E_A$ and comparing the obtained E_A with the values $E_{A,\exp}$ which are known from the experiment through Eq. (9) (shooting method). The nonlinear equation Eq. (13) was solved with the secant method, it allowed to find required E_T values with high accuracy.

The value E_A (Eq. (13)) can be calculated for any E_T in the following way. Each layer $d_1,...,d_m$ is divided into N sublayers. Let d_j is the thickness of j-th layer. Let $\xi_i=z_j+ih,\ i=0,...,N$ is the grid in this layer, h is a step, $h=d_j/N$; z_j is the left boundary of the layer. For brevity, the dependency on layer number j in these and further expressions was omitted. Then for each grid point ξ_i several iterations $1,...,k,...$ are performed:

$$\varphi_i^{(k)}=\frac{2\pi h}{\lambda}\sqrt{\left(n_{i,av}^{(k)}\right)^2-\alpha^2},\ n_{i,av}^{(k)}=\frac{1}{2}\left(n(\xi_{i-1})+n^{(k)}(\xi_i)\right),\ q_i^{(k)}=\frac{(n_{i,av}^{(k)})^2}{\sqrt{(n_{i,av}^{(k)})^2-\alpha^2}}, \tag{14}$$

$$\begin{pmatrix}u^{(k)}(\xi_i)\\ v^{(k)}(\xi_i)\end{pmatrix}=\begin{pmatrix}\cos\varphi_i^{(k)} & \left(i/q_i^{(k)}\right)\sin\varphi_i^{(k)}\\ iq_i^{(k)}\sin\varphi_i^{(k)} & \cos\varphi_i^{(k)}\end{pmatrix}\cdot\begin{pmatrix}u(\xi_{i-1})\\ v(\xi_{i-1})\end{pmatrix}. \tag{15}$$

Optics EXPRESS

$$\left|\mathbf{E}^{(k)}(\xi_i)\right| = \sqrt{\left|u^{(k)}(\xi_i)\right|^2 + \left|v^{(k)}(\xi_i)\right|^2 \frac{\alpha^2}{\left(n^{(k)}\right)^4}},\ n^{(k)}(\xi_i) = n_H + \frac{n_2\left|\mathbf{E}^{(k-1)}(\xi_i)\right|^2}{2\eta_0}. \quad (16)$$

In Eq. (16), the relation defined by Eq. (9) is taken into account. The electric field and refractive index values at the point ξ_i are therefore following:

$$E(\xi_i) = E^{(k)}(\xi_i),\ n(\xi_i) = n^{(k)}(\xi_i) \quad (17)$$

It should be noted that the intermediate iterations Eqs. (14)–(16) are performed for high index layers only.

To compare distributions of electric fields in the linear and nonlinear cases, the obtained nonlinear electric field should be scaled with respect to the amplitude of the transmitted field:

$$E(z) \to E(z)\cdot E_T, \qquad E_T = \left|\frac{2q_a u(z_a)}{2q_a u(z_a) + v(z_a)}\right| \cdot \cos\theta. \quad (18)$$

In this way, the reflectance of any multilayer coating can be calculated using Eq. (12) for any given intensity value I and any given coefficient n_2. The modulation depth values are evaluated as $\Delta R_{nl}(I) = R(I) - R_0$.

5. Determination of Kerr coefficients

In order to estimate the Kerr coefficients n_2 of Ta_2O_5 and Nb_2O_5 layers, the modulation depth values ΔR_{nl} were calculated for a series of n_2 values on the angular grid $\{\theta_j\}$ containing 101 points. The angular ranges were taken from 16.0° to 17.5° for F502 design and from 17.0° to 20.2° for F504 design. The angular ranges correspond to the reflectance levels R_0 from 92% down to 10%. Then root mean square deviation σ of model data from the experimental data (Section 3, Figs. 6(a) and 6(b)) was calculated as:

$$\sigma^2 = \left(\frac{1}{7}\sum_{i=2}^{8}\left[\Delta R_{nl}(\theta_i) - \Delta R_{ch}(\theta_i)\right]^2\right) \quad (19)$$

where θ_i values correspond to different levels of R_0, namely, 20%, 30%, 40%, 50%, 60%, 70%, 80% and 90%. The modulation depth values observed at $R_0 = 10\%$ were not taken into consideration because the spectral characteristics of the F502 and F504 samples deviate from the expected ones at the edge of the low reflection zone (see Fig. 3). The model values ΔR_{nl} were calculated assuming the intensity of the incident pulses equal to 30.9 and 75.9 GW/cm^2 for designs F502 and F504, respectively. The value of n_2 providing the minimum of σ can be considered as an estimation of the Kerr coefficient. For the samples F502 and F504, the minimum of σ were achieved with $n_2 = 2.2\cdot10^{-15}$ cm^2/W and $n_2 = 2.1\cdot10^{-15}$ cm^2/W, respectively. In Fig. 6 the experimental and model modulation depths values are compared. One can observe a very good agreement between measured and model values almost at all reflectance levels R_0. In addition, in Fig. 6 a remarkably good agreement between qualitative behavior of experimental and model data can be observed.

For the sake of cross verification of the n_2 estimation, model and experimental intensity dependent modulation depth values, $\Delta R_{nl} = R_{nl}(I) - R_0$ and $\Delta R_{ch}(I) = R_{ch}(I) - R_0$ were compared. For this purpose, ΔR_{nl} values were calculated for different intensity values using the method described above and compared with experimental values. In Figs. 5(a) and 5(b) model and experimental data are compared for

Optics EXPRESS

samples F502 and F504, respectively. For the sample F502, the comparison is plotted for $R_0 = 50\%$ and $R_0 = 80\%$. For the F504 sample, the intensity dependent modulation depth values are compared for $R_0 = 40\%$ and $R_0 = 70\%$. In both figures a good agreement between measurement and model data is observed.

In Fig. 7, the nonlinear addition $\Delta n(z)$ of the electric field distributions in the nonlinear and linear cases for the R_0 levels of 50% and 80% (Sample F502) and R_0 levels of 40% and 70% (Sample F504) are plotted.

It was experimentally demonstrated (Section 3) that along with the nonlinear effect, a thermal effect is presented. It was assumed that the modulation depth ΔR is the sum of the modulation depth ΔR_{nl} caused by the nonlinear Kerr effect and $\Delta R_{thermal}$ induced by the thermal effect:

$$\Delta R(I) \approx \Delta R_{nl}(I) + \Delta R_{Thermal}(P, \Delta t) \tag{20}$$

It is highlighted in Eq. (20) that the thermal shift of the reflectance depends on the incident power and the temperature while the nonlinear effect depends on the intensity only. The thermal shift in its turn was be estimated as:

$$\Delta R_{Thermal} = R(d_1 + \alpha_H \Delta t, d_2 + \alpha_L \Delta t, \ldots; n_H + \beta_H \Delta t, n_L + \beta_L \Delta t) - R_0 \tag{21}$$

where α_H and α_L are thermal expansion coefficients, β_H and β_L are thermo-optic constants of Ta_2O_5/Nb_2O_5 and SiO_2, respectively (see Table 1). In Fig. 6 the experimental modulation depth values ΔR_{exp} and model values ΔR calculated with the help of Eqs. (20)–(21) are compared. One can observe a good agreement between experimental and model data. This agreement confirms the validity of the developed method and demonstrates the good accuracy of determined Kerr coefficients n_2 of Ta_2O_5 and Nb_2O_5 thin film materials. It should be mentioned that the obtained n_2 value for Ta_2O_5 is consistent with the value of $2.57 \cdot 10^{-15}$ [21] and of the same order with the value of $7.23 \cdot 10^{-15}$ estimated for the waveguides at the wavelength of 800 nm [32]. The value n_2 for Nb_2O_5 is consistent with the value of $2.14 \cdot 10^{-15}$ provided in [21].

6. Conclusions

Dielectric edge filters exhibiting extremely narrow transition zone in reflectance were produced and optically characterized. The comprehensive study of the nonlinear properties of the fabricated coatings was possible due to high sensitivity of filters' spectral characteristics to any changes of the refractive indices. Measurements of the intensity dependent coatings' reflectance at a laser system emitting ultrashort pulses reveal the presence of nonlinear Kerr effect in the produced coatings. In order to quantify this effect, a new numerical method for calculation of nonlinear response of multilayer optical coatings was developed for the first time. The method evaluates modulation depth values in cases when the multilayer coating interacts with short laser pulses. The method is universal since it can be applied to any type of dielectric optical coatings and to wide spectra of laser pulses. Excellent agreement between the results of model calculations and experimental data validates the numerical method as well as the reliability of the determined Kerr coefficient of Ta_2O_5 and Nb_2O_5 thin film materials. The new method paves the way towards dielectric optical elements with engineered nonlinear optical properties for a variety of applications.

Funding

This work was supported by the DFG Cluster of Excellence, "Munich Centre for Advanced Photonics," (http://www.munich-photonics.de). T. Amotchkina has received funding from the European Union's Horizon 2020 research and innovation programme under the Marie Skłodowska-Curie agreement No 657596.

Optics EXPRESS

Acknowledgments

The authors thank Prof. F. Krausz for valuable discussion and permanent support of this work. The authors also thank D. Ehberger, Bo-Han Chen, Dr. A. Ryabov, Dr. Y. Morimoto and Dr. P. Baum for providing and maintaining the laser source. The authors are grateful to K. Fritsch and Dr. O. Pronin for fruitful discussions.